مجلة العلوم البحثة والتطبيقية
Journal of Pure & Applied Sciences
www.Suj.sebhau.edu.ly ISSN 2521-9200
Received 05/01/2018 Revised 02/02/2018 Published online 14/02/2018

Tin doping effect on properties of sprayed In_2S_3 films

*Mabrouk Kraini[1] , Ftema W. Aldbea[2], Noureddine Bouguila[1], Carlos Vázquez-Vázquez[3]
[1] Laboratory of Physics of Materials and Nanomaterials Applied at Environment (LaPhyMNE), Gabes University, Faculty of Sciences in Gabes, 6072, Tunisia.
[2] Physics department, Faculty of Science, Sebha University, Libya
[3] Laboratory of Magnetism and Nanotechnology, Institute of Technological Research, Universidade de Santiago de Compostela, 15782 Santiago de Compostela, Spain.
*Corresponding author: mabrouk.kraini@fsg.rnu.tn

Abstract Tin doped In_2S_3 films have been prepared by the spray pyrolysis (CSP) technique on glass substrates at 350 °C. The Sn doping level was changed with Sn:In (0-2 % in solution). The structural studies reveal that the deposited films are polycrystalline in nature exhibiting cubic structure. The crystallite size decreases from 23.3 to 21 nm and RMS roughness values increases from 16 to 31 nm. The transmission coefficient is about 65-70% in the visible region and 75-90 % in near-infrared region. The band gap energy increases from 2.68 to 2.83 eV for direct transitions. The refractive index values of In_2S_3:Sn thin films decrease from 2.45 to 2.40 and the extinction coefficient values are in the range 0.01-0.21.
Keywords: Morphological proprieties, Optical properties, Thin films; Sn doped In_2S_3 ; Spray pyrolysis, Structural properties.

تأثير التطعيم بالقصدير على خواص رقائق رذاذ كبريتيد الانديوم(In_2S_3)

*المبروك الكراياني[1] و افطيمة الضبيع[2] و نور الدين بوغويلة[1] و كارلوس فازكيس[3]
[1] مختبر فيزياء المواد والمواد النانوية المطبقة في البيئة (La Phy MNE) – جامعة قابس – كلية العلوم في قابس، تونس
[2] قسم الفيزياء – كلية العلوم – جامعة سبها، ليبيا
[3] مختبر المغناطيسية وتكنولوجيا النانو – معهد البحوث التكنولوجية –جامعة سانتياغو دي كومبوستيلا ،إسبانيا
* للمراسلة: mabrouk.kraini@fsg.rnu.tn

الملخص حضرت رقائق كبريتيد الانديوم المطعمة بالقصدير باستخدام طريقة الرش بالرذاذ على ركيزة زجاجية عند درجة حرارة 350 درجة مئوية. تغيير مستوى التطعيم بالقصدير (Sn) الى الانديوم (Sn : In) بنسبة 20% في المحلول. أعطت التحاليل التركيبية أن الرقائق المرسبة لها طبيعة متعددة التكلس (كريستالات) التي تظهر تركيبة المكعب. حجم التكلس يقل من 23.3 الى 21nm و وقيم خشونة RMS تزداد من 16 الى 31 nm . قيم معامل الانتقال للرقائق المحضرة كانت حوالي 65– 75 %في حدود منطقة الضوء المنظور، وايضا 75– 90 % في حدود منطقة الاشعة تحت الحمراء. للانتقالات المباشرة، لوحظ ازدياد في حزمة فجوة الطاقة من 2.68 eV الى 2.83 eV . قيم معامل الانكسار للرقائق من In2S3: Sn انخفضت من 2.45 إلى 2.40 وسجلت قيم معامل الفناء في المدى 0.01–0.21.

الكلمات المفتاحية: الخصائص المورفولوجية، الخصائص الضوئية، الرقائق، Sn مطعم In_2S_3، الرش بالرذاذ، الخصائص التركيبية.

Introduction

Over the last decade, indium sulphide (In_2S_3) is one of the potential materials for various applications [1-6]. This becomes possible due to the stability and wide band gap (2.0–3.7 eV) [7]. Furthermore, indium sulphide is a potential substitute of toxic CdS as a buffer layer in photovoltaic solar cells [8].Various techniques have been developed to synthesize In_2S_3 such as spray pyrolysis [9, 10], ultrasonic dispersion [11], chemical bath deposition [12], physical vapor deposition [13], vacuum thermal evaporation [14], etc.. Among these methods, spray pyrolysis is selected in this study because it allows preparing In_2S_3 in large area thin films at low cost.

Indium sulfide, a typical III-VI compound semiconductor, is known to exist in three polymorphs at atmospheric pressure: α, β and γ [9,10]. Of these, β-In_2S_3 is the thermodynamically stable form with tetragonal or cubic crystal structure at room temperature with a high degree of tetrahedral and octahedral vacancy sites [11-12]. In_2S_3 is an *n*-type semiconductor exhibiting excellent optoelectronic performances because of its defected spinel structure. Due to a large number of cation vacancies, one of the efficient ways of improving the properties of indium sulfide films is the addition of certain dopants

In this work, we report the influence of Sn doping on the structural, morphological and optical properties of In_2S_3 films.

2. Experimental details

The In_2S_3 thin films were prepared by spraying an aqueous solution of indium chloride ($InCl_3$) and thiourea ($CS(NH_2)_2$) in a ratio of S:In = 2.5. Tin chloride ($SnCl_4$), used as Sn source, was added to the spray solution in a controlled way. The tin to indium molar ratios (Sn:In) were varied

from 0 to 2% in the spray solution. Air compressed was used as a carrier gas at a flow rate of 6l/min. The substrate temperature was maintained at 350 °C within an accuracy of ± 5 °C.

X-ray diffraction (XRD) studies of the films were performed using monochromatic Cu-Kα radiation (1.5406 Å) (*Bruker D8 Advance diffractometer*). The film surfaces were characterized by atomic force microscope using XE-100 instrument (*Park Systems Corporation*) in non contact mode (*NC-AFM*). Microstructures and chemical compositions of the films were studied by field emission scanning electron microscope (*Zeiss FESEM Ultra PLUS*). The absorption and transmission spectrum were taken from Shimadzu UV 3101 PC spectrophotometer.

3. Results and discussion

3.1. Structural characterization

The XRD patterns of films with different values of molar ratio Sn:In from 0 to 2% are shown in Fig. 1. As it is seen, all films are polycrystalline and all the crystallographic peaks belong to the cubic β-In_2S_3 phase with diffractions from (111), (220), (311), (222), (400), (511) and (440) planes, according to JCPDS card no. 32-0456. No other phases corresponding to Sn impurity are observed which indicate that Sn ions occupy substitutional positions and did not change the crystalline system.

In these cases, with increasing the doping concentration the diffractogramms show a slight shift of (311) peak from 27.614° for undoped In_2S_3 to 27.630° for Sn:In=2%. Such behavior is attributed to the residual stress in the film caused by the difference in ionic size between Sn^{4+} (0.69 Å) and In^{3+} (0.80 Å). This is confirmed by lattice parameter *a*, which is less than the standard value which is a strong indication of stress in the films.

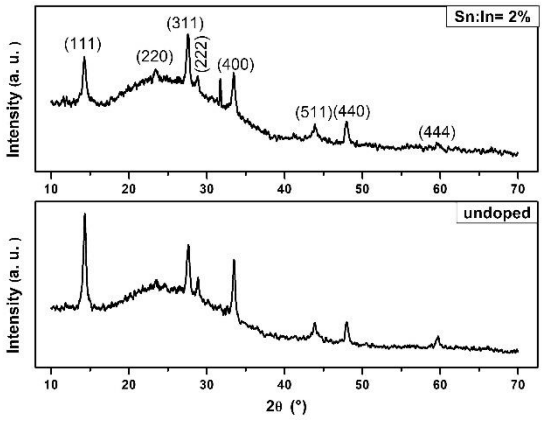

Fig. 1: XRD patterns of In_2S_3:Sn thin films.

A rough estimate of the crystallite size (D) is estimated from (311) principal peak by using the Scherrer formula [15]:

$$D = \frac{0.9\lambda}{\beta \cos\theta} \qquad (1)$$

where β is the full width at half maximum in radians, λ is the wavelength of X-ray, θ is the Bragg angle.

The calculated crystallite size decreases from 23.3 nm to 21 nm with increasing tin concentration. This trend suggests that the Sn dopant created new nucleation centers, which in turn, may have changed the nucleation type from homogeneous to heterogeneous [16].

3. 2. Morphological characterization

Figure 2 exhibits the scanning electron micrographs of the samples. As seen, the surface morphology of the films depends on the Sn:In molar ratio. The surface of the samples revealed continuous films with no cracks and voids and it is clearly seen also from the FESEM photographs that the films are dense without pinholes and perfectly covering the entire substrates for all Sn:In molar ratios.

Figure 3 shows 2D and 3D NC-AFM images (2μm-2μm) of In_2S_3:Sn thin films for different Sn:In molar ratios. These images show that the surface morphologies of the films are dependent on the Sn doping. The films were well covered, homogeneous, dense and continuous. The RMS roughness values increses from 16 to 31 nm with increasing Sn doping.

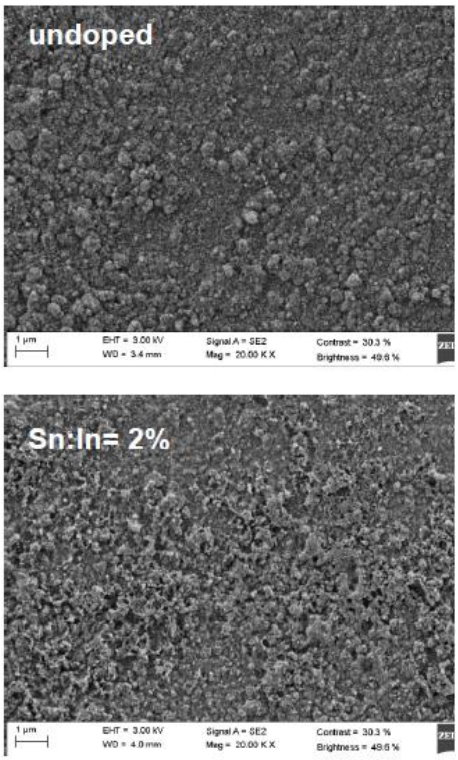

Fig. 2: FESEM images of In_2S_3 thin films for different Sn doping

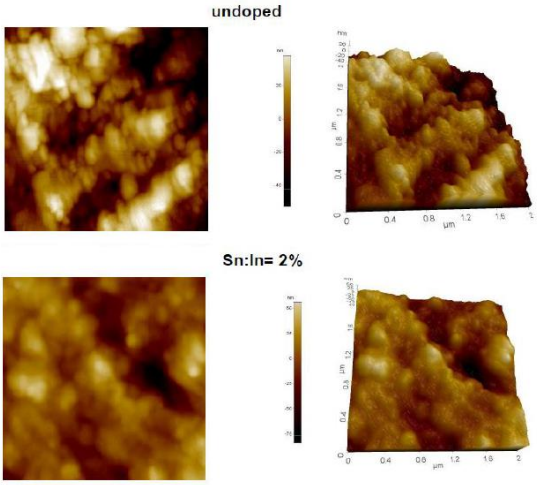

Fig. 3: NC-AFM images of In_2S_3 thin films for different Sn doping.

3.3. Optical Characterization

The spectra of absorbance and transmittance measured in the wavelength range 300–2400 nm of the films of In_2S_3:Sn for various molar ratios Sn:In are shown in figure 4a and b, respectively.

One can see from the transmittance value that the UV radiations are completely absorbed (fig.4a). The transmittance decreases after the doping and there is a shift of the fundamental absorption towards shorter wavelengths. The transmission coefficient increased of about (65-70%) in the visible range and in the near infrared (70-90%) with a linear absorption edge in the neighborhood of the ultraviolet (UV) region.

The region of strong absorption is the fundamental absorption (λ <450 nm) in the film due to the interband electronic transitions. The absorption edge (fig.4b) of Sn doped In_2S_3 films deposited for different doping concentrations shifts to a lower wavelength.

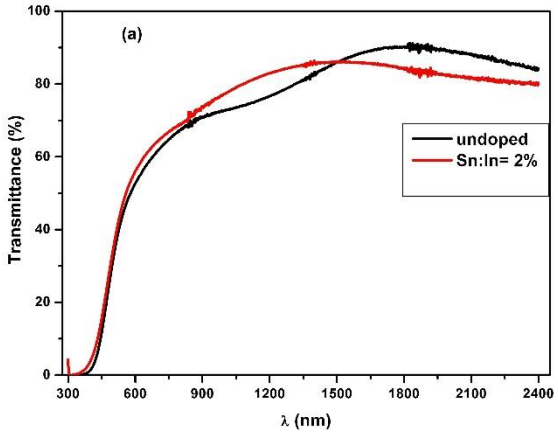

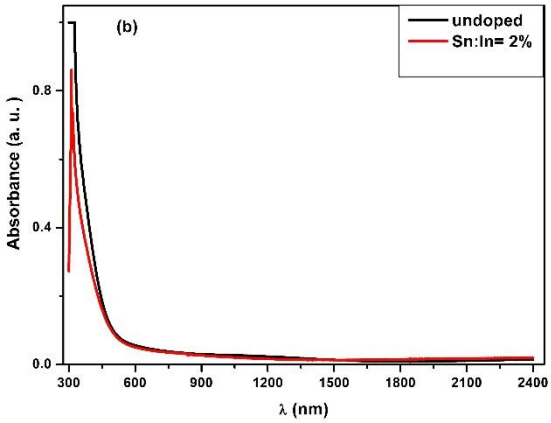

Fig. 4: Transmittance (a) and absorbance (b) spectra of In_2S_3:Sn thin films.

The absorption coefficient (*α*) of the films can be estimated by the equation [17]:

$$\alpha = \frac{2{,}303}{d} A \quad (2)$$

where d = 300 nm is the thickness of the prepared thin films, A is the absorbance.

The variation of the absorption coefficient of In_2S_3:Sn thin films with wavelength for different concentrations of Sn is shown in figure 5. We can notice that α in general decreases with increasing wavelength. It can be seen that the value of α is in the order of 10^4 cm^{-1}. It can be seen that the absorption through of In_2S_3:Sn films are relatively high at below band gap region indicating a high concentration of free carriers. The higher values of the absorption is attributed to that the incoming photons have the sufficient energy to excite the electrons from the valence band to the conduction band. It was also noted that the absorption edge was not sharp for the doped samples indicating absorption in longer wavelength region also. This might be due to the introduction of shallow donor levels due to the doping. These results are consistent with literature [18- 20]. The absorption decreases in the higher wavelength region and this decrease is corresponds to the reduction in the photon's energy.

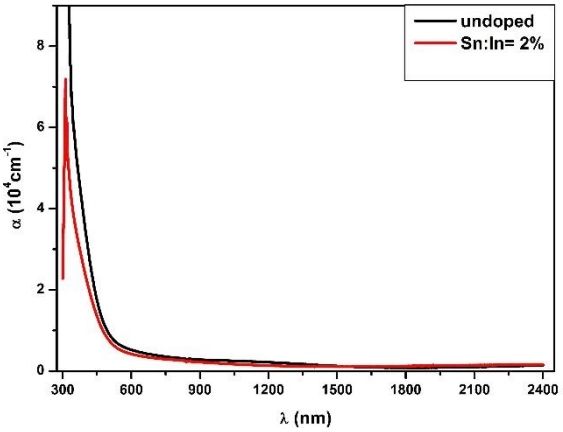

Fig.5: Absorption coefficient of In_2S_3:Sn thin films.

The extinction coefficient (*k)* is given by the following expression [21]

$$k = \frac{\lambda\alpha}{4\pi}$$

(3)

On Fig. 6, we studied the evolution of the extinction coefficient according to the wavelength of the In_2S_3 films doped with tin. The values of *k* are high in the zone of strong absorption and vary slightly according to the quantity of tin in the films. Moreover, the *k* values are in the range 0.01-0.21 for all wavelengths.

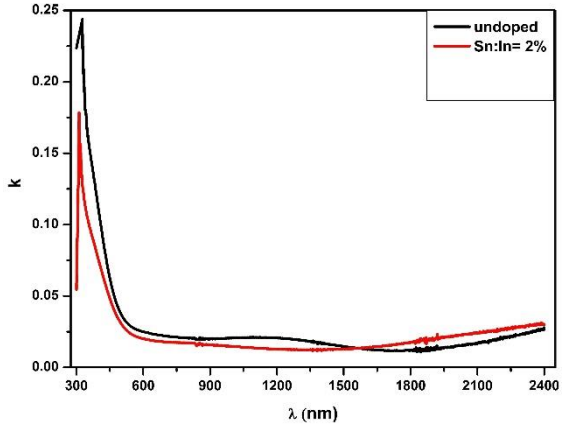

Fig.6: Extinction coefficient of In_2S_3:Sn thin films.

The optical band gap of the films is determined by the following relation [18]

$$\alpha h\nu = A(h\nu - E_g)^{1/2}$$

(4)

where *A* is a constant, *h* is the Planck constant, υ is the frequency and E_g is the optical band gap.

The value of $(\alpha h\nu)^2$ is plotted as a function of the incident photon energy (hν) in figure 7. Then, the value of (hν) at $(\alpha h\nu)^2 = 0$, obtained by extrapolation, is the optical energy band gap.

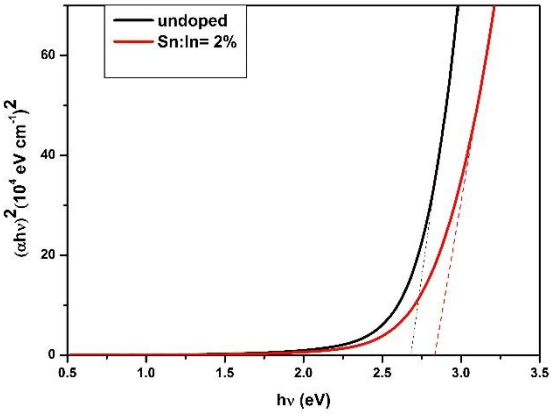

Fig.7: Variation of $(ahv)^2$ versus photon energy for In_2S_3:Sn films.

The calculated values of the E_g of In_2S_3:Sn thin films as a function of Sn:In molar ratio are listed in table 2. An increase of the E_g values as the tin content increases is evident, from 2.68 to 2.83 eV. Moreover, the E_g could also be influenced by the variation of particle size with Sn doping which is in the nanometer range, though it is not close to the Bohr radius. Therefore in the current study, the reduction in the particle size could contribute to the increase of E_g of the films with the increase of Sn:In molar ratio. These results are agreement with the literature [7, 22-24]. Such an increase of optical energy gap is useful for photovoltaic applications since it increases the collection of photons in the ultraviolet range [25].

Various empirical and semi-empirical rules are available to correlate refractive index (*n)* and E_g. Among them, the Herve–Vandamme relationship for *n* and E_g is [26]:

$$n^2 = 1 + \left(\frac{A}{E_g + B}\right)^2$$

(5)

where *A* and *B* are constants (*A = 13.6 eV and B = 3.4 eV*).

The calculated *n* and E_g values of In_2S_3 thin films obey to the above said relations. The values of *n* of In_2S_3:Sn thin films decrease from 2.45 to 2.40 with increasing Sn:In molar ratio which may be attributed to the variation in packing density of the films. Indeed, this reduction is accompanied by a small increase in transmission. These results are comparable to that found in the literature [19,26-28]. Since n is strongly connected with band gap energy. Therefore,
larger band gap energy has a smaller value of *n*.

4. Conclusion

In summary, In_2S_3 thin films doped by tin were carried out by CSP technique with different Sn:In molar ratios. The structural, morphological and optical properties of In_2S_3:Sn thin films have been studied in this work. The prepared films are polycrystalline and exhibit a cubic β-In_2S_3 phase. The crystallite size decreased from 23.3 to 21 nm with Sn doping. According to FESEM, the surface morphology of the films is continuous and free of cracks. RMS roughness increased from 16 to 31 nm. In_2S_3:Sn films exhibit transparency over 65-70% in the visible region and 75-90 % in near-infrared region. The values of E_g are found to vary in the range 2.68–2.83 eV for direct transitions. The *n* values of In_2S_3:Sn thin films decrease from 2.45 to 2.40 and the *k* values are in the range 0.01-0.21.

References

[1]- A. A. El Sbazly, D. Abd Elhady, H. S. Metwally, M. A. M. Seyam, *J. Phys.: Condens. Matter* 10 (1998) 5943-5954.
[2]- M. Kilani, B. Yahmadi, N. K. Turki, M. Castagné, *J. Mater. Sci.* 46 (2011) 6293-6300.
[3]- K. Hara, K. Sayama, H. Arakawa, *Sol. Energy Mater. Sol. Cells* 62 (2000) 441-447.
[4]- R. Nomura, S. Inazawa, K. Kanaya, H. Matsuda, *Appl. Organomet. Chem.* 3 (1989) 195-197.
[5]- E. Dalas, L. Kobotiatis, *J. Mater. Sci.* 28 (1993) 6595-6597.
[6]- Y. He, D. Li, G. Xiao, W. Chen, Y. Chen, M.

Sun, H. Huang. X. Fu, *J. Phys. Chem. C* 113 (2009) 5254-5262.
[7]- N. Barreau, *Solar Energy* 83 (2009) 363-371
[8]- D. Braunger, D. Hariskos, T. Walter, H. W. Schock, *Sol. Energy Mater. Sol. Cells* 40 (1996) 97-102.
[9]- S. Cingarapu, M. A. Ikenberry, D. B. Hamal, C. M. Sorensen, K. Hohn, K. J. Klabunde, *Langmuir* 28 (2012) 3569-3575.
[10]- L. J. Liu, W. D. Xiang, J. S. Zhong, X. Y. Yang, X. J. Liang, H. T. Liu, W. Cai, J. *Alloys Compd.* 493 (2010) 309-313.
[11]- Z. Li, X. Tao, Z. Wu, P. Zhang, Z. Zhang, *Ultrason. Sonochem.*16 (2009) 221-224
[12]- H. Spasevska, C. C. Kitts, C. Ancora, G. Ruani, *Int. J. Photoenergy* 2012 (2011) 1-7.
[13]- A. Akkari, C. Guasch, M. Castagne, N. Ka. Turki, J. Mater. Sci. 46 (2011) 6285-6292
[14]- A. Timoumi, H. Bouzouita, B. Rezig, *Thin Solid Films* 519 (2011) 7615-7619.
[15]- B. D. Cullity, Elements of X-ray Diffraction, Addison-Wesley, Reading, MA 1978.
[16]- A. Mhamdi, B. Ouni, A. Amlouk, K. Boubaker, M. Amlouk, *J. Alloys Compd.* 582 (2014) 810-822
[17]- G. B. Kamath, C. M. Joseph, C. S. Menon, *Mater. Lett.* 57 (2002) 730-733.
[18]- M. Kraini, N. Bouguila, I. Halidou, A. Timoumi, S. Alaya, *Mater. Sci. Semicond. Process.* 16 (2013) 1388-1396.
[19]- S. P. Nehra, S. Chander, A. Sharma, M. S. Dhaka, *Mater. Sci. Semicond. Process.* 40 (2015) 26-34.
[20]- M. H. Suhail, S. G. Kaleel, F. M. Yasser, *Asia Pac. j. res.* 1 (2014) 80-95
[21]- S. Rajeh, A. Mhamdi, K. Khirouni, M. Amlouk, S. Guermazi, *Opt. Laser Technol.* 69 (*2015)* 113-121.
[22]- M. Kraini, N. Bouguila, I. Halidou, A. Moadhen, C. Vázquez-Vázquez, M. A. López-
[23]- Quintela, S. Alaya, *J. Electron. Mater.* 44 (2015) 2536-2543.
[24]- J. Koaib, N. Bouguila, M. Kraini, A. Mhamdi, I. Halidou, M. Ben Salem, H. Bouzouita, S. Alaya, *J. Mater. Sci.: Mater. Electron.* 27 (2016) 9216–9225.
[25]- M. Kraini, N. Bouguila, J. Koaib, C. Vázquez-Vázquez, M. A. López-Quintela, S. Alaya, *J. Electron. Mater.* 45 (2016) 5936-5947
[26]- C. Guillén, T. Garcia, J. Herrero, M. T. Gutiérrez, F. Briones, *Thin Solid Films* 451 (2004) 112-115
[27]- P. J. L. Herve, L. K. J. Vandamme, *J. Appl. Phys.* 77 (1995) 5476-5477.
[28]- M. M. El-Nahass, B. A. Khalifa, H. S. Soliman, M. A. M. Seyam, *Thin Solid Films* 515 (2006) 1796-1801.
[29]- A. Timoumi, H. Bouzouita, B. Rezig, *Aust. J. Basic Appl. Sci.* 7 (2013) 448-456.